Supporting information

Preparation of TiO_2 (P25) photoanode

A paste of anatase TiO_2 was prepared by mixing 200 mg of TiO_2 powder (P25, Degussa), 30 µl of acetylacetone, 400 µl of water, and 1 drop of Triton X-100. The paste was painted on conducting glass (FTO; Fluorine doped tin oxide, 20 × 15 mm^2, Nippon Sheet Glass Co. Ltd.) using the squeegee method. The bottom area (ca. 15 mm × 15 mm) of the FTO was covered with TiO_2, but not the top side of the FTO to allow for contact. The samples were calcined at 823 K for 30 minutes in air. The electrode was subsequently treated with $TiCl_4$ for particle-necking. 100 mM $TiCl_4$ solution was applied on the surface of electrode covered with TiO_2, and then calcined at 823 K for 30 minutes. The top side of the sample was then contacted with Cu wire using In solder, and the contact of electrode was insulated with silicone rubber.

Quantitative determination of formate

The amount of $HCOO^-$ was determined using an ion chromatograph (ICS-2000, Dionex Corporation) with IonPacAS15 and IonPacAG15 columns. The detector is conductometric detection. The column temperature was maintained at 308 K. A 3 mM KOH solution was used as the first eluent for 10 minutes. The eluent was then gradually changed to a 10 mM KOH solution for the next 5 minutes, after which the eluent was gradually changed to a 60 mM KOH solution for the next 10 minutes.

The calibration curve was obtained using HCOOH solutions with different concentration (0.01mM, 0.05mM, 0.1mM, 0.2mM and 0.5mM). HCOOH solutions for calibration were prepared by diluting HCOOH with 0.1 M $NaHCO_3$ aqueous solution mixed with phosphoric acid which is same as the electrolyte of CO_2 photoreduction experiment (HCOOH-EL). The calibration curve was measured in the start of every experiment. We also checked the calibration curve using HCOOH solutions prepared by diluting HCOOH with deionized water (HCOOH-DW). When HCOOH-EL solution was used for calibration, the peak shape of chromatograph was broad compared with that obtained using HCOOH-DW because of the high concentration of cation in HCOOH-EL. However, we confirmed that the calibration curve was same for both cases. The accuracy of the measurement is ±5%.

Spectrum of solar simulating light

A solar simulator (HAL-320, Asahi Spectra Co., Ltd.) was used as the light source. A branched optical fiber was used to split the light in two, and the intensities of the two split light beams were adjusted to 1 SUN (Air Mass 1.5 (AM1.5)) using a 1 SUN checker (CS-20, Asahi Spectra Co., Ltd.). The spectrum of the light irradiated through the fiber was measured by utilizing a spectrometer (LS-100, EKO Instruments). The results are shown in Figure S1. The spectrum approximately

corresponded to the standard AM 1.5 spectrum, especially in the wave region from 350 nm to 800 nm.

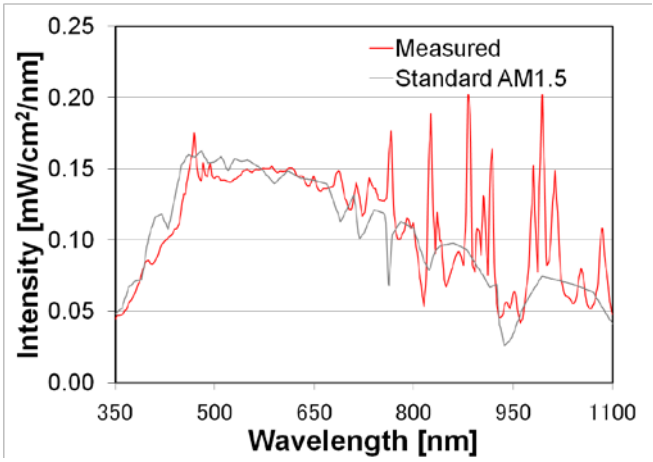

Figure S1. Spectrum of the solar simulating light.

Photoresponse of r-STO photoanode

The transmission spectra of the r-STO and STO were measured using a UV-VIS-NIR spectrophotometer (UV-3600, SHIMADZU). The results are shown in Figure S2. The light absorption edge of STO was observed around 380 nm which corresponds to the previous study. The transmittance of STO observed in the visible light region (380 nm < λ < 800 nm) was very low because the STO used in this study was opaque. Therefore, light scattering occurred over the STO. Furthermore, the r-STO showed the same light absorption edge as the STO and the transmittance in the visible light region was lower than in STO. The r-STO showed a dark blue color caused by the reduction of Ti^{4+}. Therefore, the r-STO absorbed visible light.

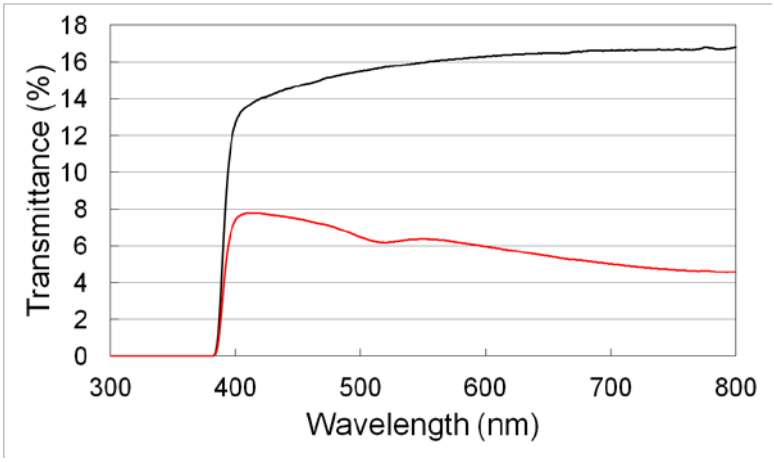

Figure S2. Transmission spectra of r-STO (red line) and STO (black line)

The current-potential characteristics of r-STO under visible light irradiation were evaluated in the

three electrode configuration. The solar simulator equipped with a UV cut filter (λ > 400 nm) was used as the light source. The r-STO showed no photoresponse under visible light irradiation as shown in Figure S3. The r-STO showed light absorption even in the visible light region as seen in Figure S2. However, r-STO could not utilize the visible light to generate a photocurrent. Therefore, it was confirmed that the photoresponse of r-STO corresponds to that of bare STO (Bandgap: 3.2 eV).

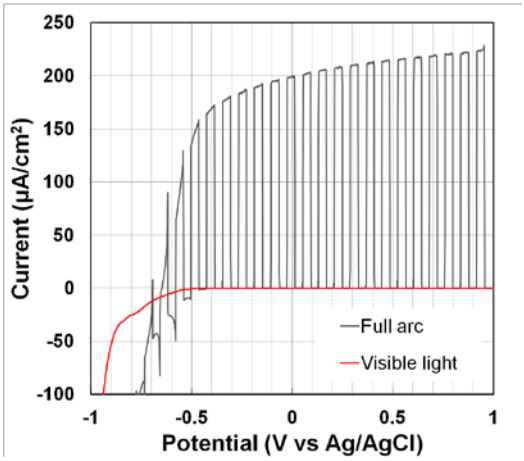

Figure S3. Photoresponse of r-STO under visible light irradiation (LUX422, > 400 nm, red line) and full arc irradiation (gray line)

In the previous study,[24] light was irradiated from the TiO_2 (P25) photoanode side, and InP/[RuCP] photocathode was irradiated with light transmitted through the translucent TiO_2 (P25) photoanode and proton exchange membrane. However, if the r-STO photoanode is used as a photoanode, the visible light to irradiate the InP/[RuCP] photocathode will be drastically decreased by the absorption and scattering of light over r-STO. Furthermore, the available wavelengths for r-STO and InP/[RuCP] could be completely separated into UV and visible light, respectively. Therefore, from the viewpoint of efficient utilization of the light, the light was split into UV and visible light by utilizing a branched optical fiber and a UV-cut filter to irradiate r-STO and InP/[RuCP], respectively. To simulate this condition, the intensity of both split light beams were adjusted to 1 SUN (Air Mass 1.5 (AM1.5)) using a 1 SUN checker (CS-20, Asahi Spectra Co., Ltd.), respectively. r-STO photoanode was irradiated with direct light from the fiber, and the InP/[RuCP] photocathode was irradiated with light from another fiber equipped with a UV-cut filter (LUX422, Asahi Spectra Co., Ltd., λ > 400 nm). The transmitted light through the r-STO photoanode was intercepted to not irradiate the InP/[RuCP] photocathode. In this condition, the r-STO photoanode and InP/[RuCP] photocathode could utilize the UV and visible light region of the solar simulating light (1SUN, AM1.5), respectively.

Oxygen photogeneration over r-STO in the absence and presence of formic acid

The amount of photogenerated O_2 over r-STO in the absence and presence of formic acid was determined by detecting the dissolved O_2 in electrolyte using O_2 probe [1,2] (NeoFOX, FOSPOR probe). The calibration curve was obtained by two point calibration. One point is measured without dissolved O_2 under Ar atmosphere and another is the saturated point of dissolved oxygen under O_2 atmosphere (0.0285ml/ml at 1atm, 298 K). Current-time measurement was conducted in the three electrode configuration. r-STO, Ag/AgCl and glassy carbon electrode were used as the working, reference and counter electrodes, respectively. A 0.1 M phosphate buffer solution containing 0.26 mM formic acid was used as the electrolyte. The applied potential was maintained at 0V vs Ag/AgCl. At the first of experiment, the electrolyte was bubbled with Ar gas to remove the dissolved O_2. Then, light was irradiated to r-STO for 4 minutes. The photocurrent was adjusted around 1.6 ~ 1.8 mA by controlling the light intensity. After 4 minutes irradiation, light was turned off and kept for several minutes, and then Ar gas was bubbled into electrolyte to remove dissolved O_2 again.

Time profile of the amount of dissolved O_2 in electrolyte and the current observed over r-STO in the absence and presence of formic acid are shown in Fig. S4 (a) and (b), respectively. Fig. S4 (c) is a magnified figure of Fig. S4 (b). Blue line in Fig. S4 (c) indicates the theoretical amount of O_2 calculated by observed photocurrent with 100% of current efficiency. At the start of light irradiation, the amount of dissolved oxygen corresponded to the theoretical amount. A part of dissolved O_2 was moved from electrolyte to gas phase at the headspace of the reactor during the photoreaction. Therefore, the amount of O_2 detected as dissolved gas in electrolyte become lower compared with theoretical amount at the end of photoreaction.

The amount of O_2 observed in the presence of formic acid was slightly lower than that observed in the absence of formic acid. However, it was confirmed that almost all the charge was consumed to generate O_2 even in the presence of formic acid (Fig. S4 (c)). Negligible decrease in formate concentration was observed after photoreaction, while 2.19 C of charge was observed during the reaction which is enough to completely decompose the formic acid in the electrolyte (0.43 C). These results indicate that r-STO selectively oxidizes water even in the presence of formic acid.

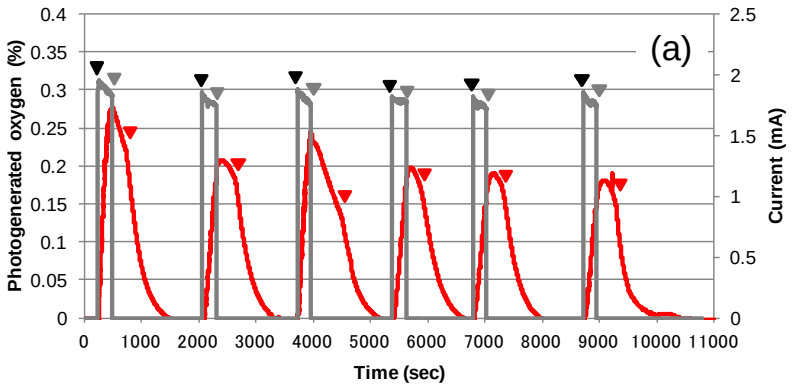

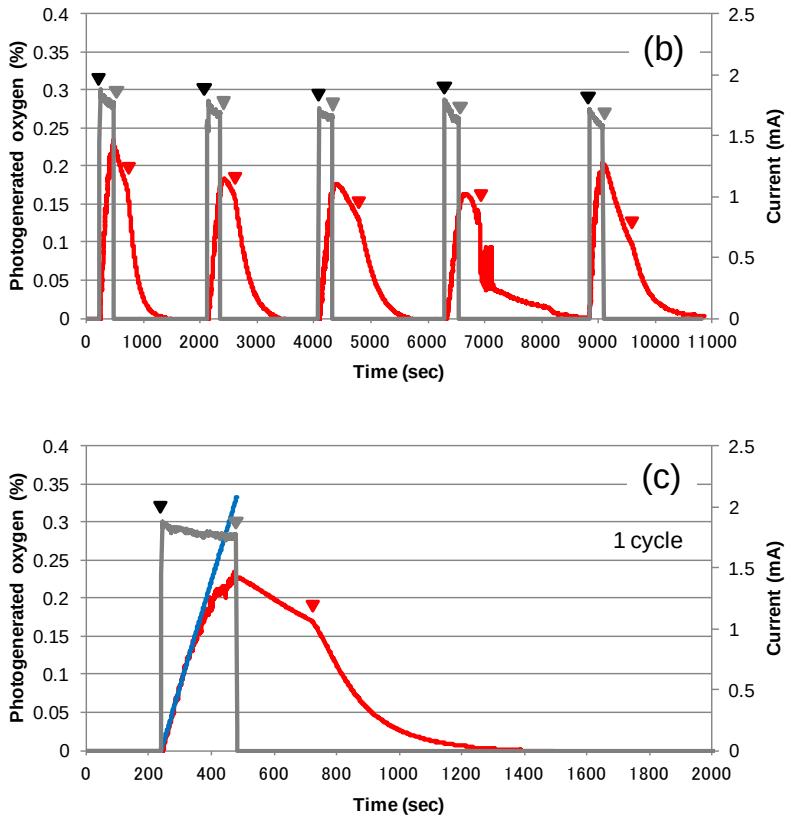

Figure S4. Time profile of the amount of dissolved oxygen (red line, left vertical axis) in electrolyte and the current (gray line, right vertical axis) observed over r-STO in the absence (a) and presence (b) of formic acid. The light was turned on (black triangle) and off (gray triangle) during the measurement. After each irradiation period, the dissolved oxygen in the electrolyte was removed by Ar bubbling (red triangle). Fig. S4 (c) is a magnified figure of Fig. S4 (b). Blue line indicates the theoretical amount of oxygen calculated by observed photocurrent with 100% of current efficiency.

Reference

1. D. K. Zhong, S. Choi and D. R. Gamelin, *J. Am. Chem. Soc.*, 2011, **133**, 18370–18377.
2. C. R. Cox, M. T. Winkler, J. J. H. Pijpers, T. Buonassisi and D. G. Nocera, *Energy Environ. Sci.*, 2013, **6**, 532-538

Current-potential characteristics of r-STO//InP/[RuCP] under solar simulating light irradiation

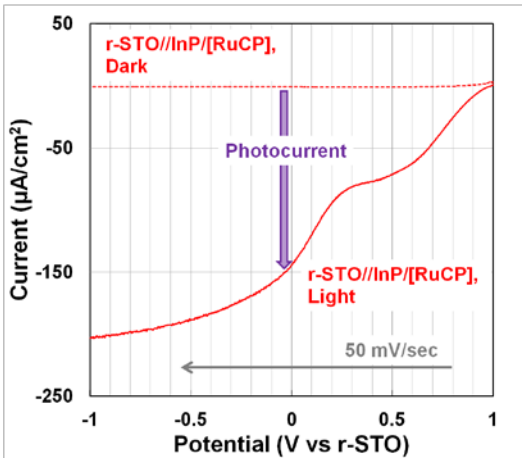

Figure S5. Current-potential characteristics of r-STO//InP/[RuCP] under solar simulating light irradiation (solid line) and dark condition (dotted line)

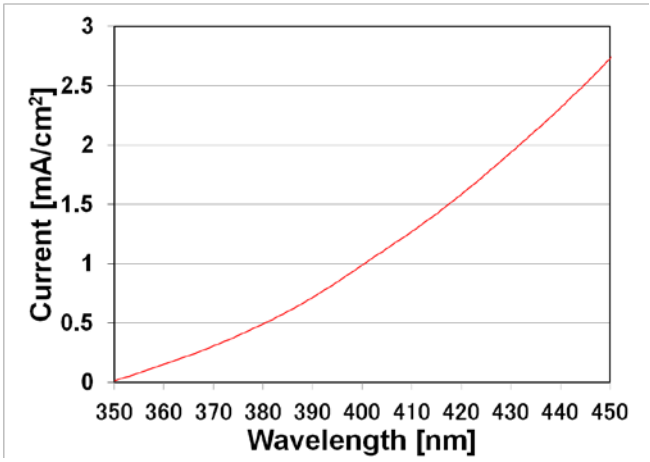

Figure S6. Expected photocurrent calculated by the spectrum of the solar simulating light hypothesizing 100% photon to current conversion efficiency. 490 μA/cm^2 of photocurrent is expected with irradiation of 350 nm < λ < 380 nm conducted without losses such as thermal relaxation.

Isotope tracer analysis utilizing $H_2{}^{18}O$ in Z-scheme system

$H_2{}^{18}O$ isotope tracer analysis was conducted to verify oxygen generation from water in the Z-scheme system reaction. 8 ml of 0.1 M $NaHCO_3$ aqueous solution containing phosphoric acid and 25% $H_2{}^{18}O$ solution was used as the electrolyte solution for the working and counter electrode sides. The electrolyte solution in the working electrode side was bubbled with Ar gas for 20 minutes to remove dissolved air, and then it was bubbled with CO_2 gas for 10 minutes before the experiment. During the experiment, CO_2 gas was continuously flowed into the working electrode side of the Z-scheme system. The counter electrode side of the Z-scheme system was used in the closed

condition. After photocatalytic reduction of CO_2, a clear peak due to $^{18}O_2$ (m/z = 36) and $^{16}O^{18}O$ (m/z = 34) was observed in the gas phase of the counter side. This result indicates that H_2O was oxidized to O_2 over the reduced $SrTiO_3$ electrode. In other words, H_2O was used as an electron donor to reduce CO_2.

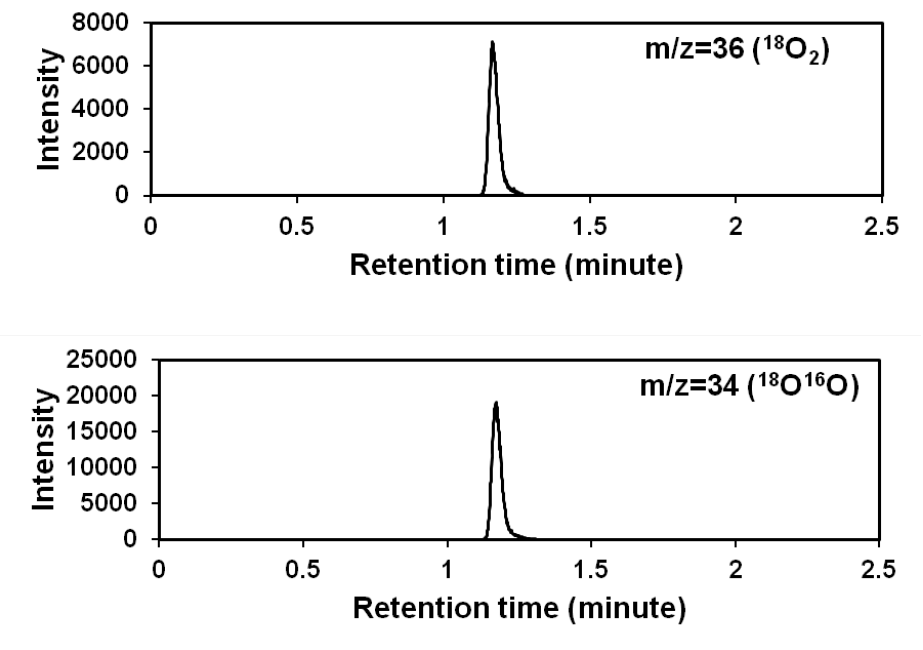

Figure S7. GC-MS spectra from tracer analysis utilizing 0.1 M $NaHCO_3$ aqueous solution containing phosphoric acid and 25% of $H_2{}^{18}O$. The spectra were calculated by subtracting the signal of air from the signal of the sample, corrected after the photocatalytic reaction in the r-STO//InP/[RuCP] Z-scheme system.

Isotope tracer analysis utilizing $^{13}CO_2$ in r-STO/InP/[RuCP] wireless devise system

$^{13}CO_2$ isotope tracer analysis was conducted to verify the carbon source of formate in the r-STO/InP/[RuCP] wireless devise system. To detect the formation of $H^{13}COO^-$ and $DCOO^-$, an ion chromatograph, interfaced with a time-of-flight mass spectroscopy system (IC-TOFMS, JEOL JMS-T100LP), was used with MeOH added as the mobile phase. 7 ml of 0.1M $NaHCO_3$ aqueous solution containing phosphoric acid was used as the reaction media. Ar gas was bubbled into the solution to remove dissolved air, and then it was bubbled with $^{13}CO_2$ gas before the experiment. During the experiment, $^{13}CO_2$ gas was continuously flowed into the solution. After photocatalytic reduction of CO_2, a clear peak due to $H^{13}COO^-$ (m/z = 46) was observed in the solution, while negligible amount of $H^{12}COO^-$ (m/z=45) was detected. This result indicates that the carbon source for formate is not from impurity organics, but CO_2 dissolved in soluition,

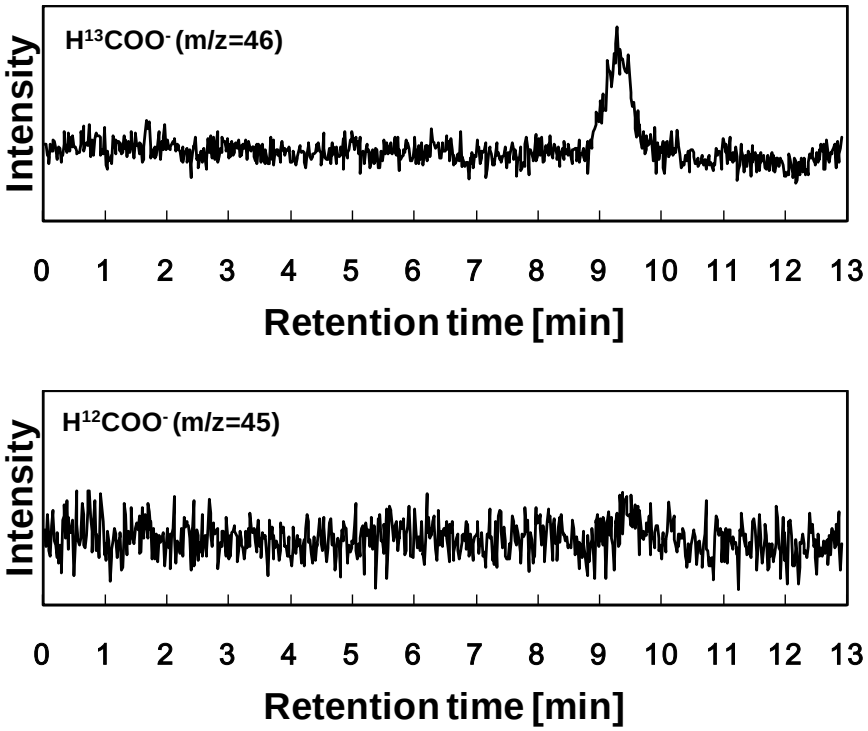

Figure S8. IC-TOFMS spectra from a tracer experiment utilizing $^{13}CO_2$.